JOURNAL OF AGRICULTURAL AND FOOD CHEMISTRY

Article

pubs.acs.org/JAFC

Structure Modification of Montmorillonite Nanoclay by Surface Coating with Soy Protein

Minfeng Jin and Qixin Zhong*

Department of Food Science and Technology, University of Tennessee, Knoxville, Tennessee 37996, United States

ABSTRACT: To achieve exfoliated and/or intercalated structures, montmorillonite (MMT) was surface-coated by soy protein at 60 °C, at MMT/soy protein powder mass ratios of 49:1, 9:1, 4:1, and 2:1 and pH 2.0−10.0. The protein-coated MMT was triple-washed and lyophilized for characterization. Protein coating was observed at all pH conditions, based on data from X-ray diffraction, Fourier transform infrared spectroscopy, zeta potential, and quantification of protein remaining in the continuous phase and present in the triple-washed MMT. At a mass ratio of 4:1, >90% protein bound with MMT, with the largest *d*-spacing at pH 9.0. When the mass ratio was increased to 2:1, protein-coated MMT at pH 9.0 demonstrated the highest degree of intercalation/exfoliation, corresponding to disappearance of the diffraction peak characteristic of pristine MMT. This study thus demonstrated that intercalation/exfoliation of MMT can be easily achieved by coating with low-cost soy protein for manufacturing nanocomposite materials.

KEYWORDS: *layered montmorillonite nanoclay, surface coating, soy protein, intercalation, X-ray diffraction*

INTRODUCTION

Concerns of fossil fuel depletion, increase of petroleum price, and negative environmental impacts of persistent petro-plastic wastes have been the driving force in investigating bioplastic packaging based on renewable, low-cost, and degradable biopolymers.[1,2] The annual growth of bioplastics has been ca. 17−20% since 2006, and the global demand for bioplastics is estimated to quadruple by 2013.[3] Companies such as Coca-Cola, Frito Lay, and Walmart have already adopted bioplastic bottles, pouches, and plastic wraps.[4]

Poly(lactic acid) synthesized from monomers derived from starch has been a dominating polymer in manufacturing bioplastics, but materials from sources such as microorganisms and algae and advanced technologies such as nanotechnology are emerging in the bioplastics industry.[3] Nanocomposites, composed of nanoscale fillers uniformly dispersed in a polymer matrix, have the promise to improve mechanical, barrier, and thermoresistance properties of natural biopolymer-based packaging films.[5−7] These properties are currently technological challenges of developing biopackaging to replace conventional petro-plastics. Montmorillonite (MMT) is one of the most popular layered silicates in developing biopolymer-based nanocomposites because of its low cost, abundance,[8,9] large surface area, and large specific aspect ratios estimated to be around 50−1000.[2,5,7]

Proteins have been extensively studied as film-forming biopolymers in the past two decades.[10−14] Protein films have lower water vapor permeability and better oxygen barrier properties than starch films.[2,7,15] However, when compared to petro-plastics, protein films have poor mechanical properties such as brittleness, rigidness, low elongation percentage, and relatively low moisture and gas resistance, but these properties can be improved by incorporation of nanoclays.[5,16,17] Studies on structure−property relationship have repeatedly illustrated that nanocomposite materials with either intercalated or exfoliated MMT nanolayers have much improved mechanical and barrier properties relative to conventional composite materials with the fillers dispersed as micrometer-sized structures.[14,18−20]

Dispersion properties of MMT particles play an important role in structural formation in nanocomposites.[21] Generally speaking, because enlarged *d*-spacing (distance between clay layer platelets) favors the entrance of polymer chains, MMT with bigger *d*-spacing is much more easily transformed to intercalated or exfoliated structures in final nanocomposites. To enlarge *d*-spacing, strategies have been developed by chemically modifying surface properties of MMT or physically coating MMT with molecules.[21−23] Intercalation agents have been studied for amino acids, primary aliphatic amines, and quaternary ammonium[21] and sequential steps of hydrochloric acid and bovine serum albumin.[24] The prior exfoliated or intercalated MMT structures can then be used to produce nanocomposite materials, with the possibility to maximize the extent of exfoliation/intercalation of MMT to improve mechanical and barrier properties.

The affinity of proteins and amino acids on soil minerals is well-established,[25,26] implying the possibility of surface coating MMT with naturally occurring low-cost proteins for direct exfoliation/intercalation. The objective of this work was thus to study the feasibility to directly surface-coat MMT by soy proteins (SP) to increase the *d*-spacing and obtain the intercalation and/or exfoliation of MMT layers. In addition to the mass ratio of MMT/SP, experiments were conducted at different pH conditions that are expected to directly affect surface properties of MMT and SP based on electrostatic interactions.

Received: May 3, 2012
Revised: September 26, 2012
Accepted: November 19, 2012
Published: November 19, 2012

dx.doi.org/10.1021/jf301934j | J. Agric. Food Chem. 2012, 60, 11965−11971

MATERIALS AND METHODS

Materials. Na^+-MMT (Cloisite Na^+ Nanoclay) was purchased from Southern Clay Products, Inc. (Gonzales, TX, USA). According to the manufacturer, the MMT product had a cation exchange capacity of 92.6 mequiv/100 g, a moisture content below 2.0%, a particle size of 10% smaller than 2.00 μm, 50% smaller than 6.00 μm, and 90% smaller than 13.0 μm, and an X-ray diffraction d-spacing (001) of 1.2 nm. Defatted soy flour (catalog no. 960024, with 50.30% protein according to the manufacturer) was a product from MP Biomedicals, LLC (Solon, OH, USA). Bovine serum albumin (BSA) and BCA Protein Assay Reagent A were ordered from Pierce Biotechnology (Rockford, IL, USA). Other chemicals such as acid, base, and salts were from Thermo-Fisher Scientific Inc. (Fair Lawn, NJ, USA) or Sigma-Aldrich Corp. (St. Louis, MO, USA). Chemicals were used as received.

Extraction of Soy Protein. SP was extracted from soy flour using the protocol of preparing SP isolate.[27] Soy flour after further size reduction with a coffee grinder (Hamilton Beach Proctor-Silex, Inc., Southern Pines, NC, USA) was suspended in deionized water at a solid/liquid mass ratio of 1:10, adjusted to pH 9.0 using 4 N NaOH, and heated to 48 °C for 3 h of extraction using a magnetic stirring hot plate (model Isotemp, Fisher Scientific). The extract was separated by centrifugation (Sorvall RC 5B Plus, Newtown, CT, USA) at 3778g for 15 min at ambient temperature (23 °C), followed by sequential filtering with no. 1 and 2 filter papers (Whatman, Lawrence, KS, USA) twice. The same batch of soy flour powder was extracted three times to improve the protein extraction productivity. The three filtrates were combined and acidified to pH 4.5 by using 6 N HCl, and the precipitated SP was separated by centrifugation at 3778g for 30 min at 23 °C. The precipitate was redispersed in deionized water, adjusted to pH 9.0, and reprecipitated at pH 4.5. The reprecipitation was repeated two additional times to remove impurities. The final precipitate was resuspended, neutralized for acidity, and spray-dried using a B-290 mini spray-dryer (Büchi Labortechnik AG, Flawil, Switzerland) at inlet and outlet temperatures of 150 and 55−65 °C, respectively, and a feed rate of 6.67 mL/min. The spray-dried soy protein powder (SPP) was collected and stored at −20 °C in a freezer.

Surface Coating of MMT. MMT was surface-coated by SP using a solution intercalation method[18] with modifications of MMT/SPP mass ratio and pH. Two groups of experiments were performed to investigate the effects of MMT/SPP mass ratio and coating pH. The first group was conducted at pH 2.0−10.0 at a MMT/SPP mass ratio of 4:1. In the second group, MMT/SPP mass ratios of 49:1, 9:1, 4:1, and 2:1 were studied at the pH identified from the first group. Briefly, SPP and MMT dispersions were prepared separately in 10 mM NaH_2PO_4 buffer according to the mass ratio, adjusted to a desired pH, and preheated to 60 °C. The MMT dispersion was slowly added into the SPP dispersion while being mixed at 1000 rpm using a magnetic stirring hot plate. The slurry was agitated at the same speed for 3 h with the temperature maintained at 60 °C. After centrifugation at 3778g for 15 min at 23 °C, the supernatant was collected, and the precipitate was resuspended in the same volume of fresh buffer to remove the unbound and loosely bound proteins. The washing step was repeated three times, and the supernatants were combined and centrifuged at 10000g for 30 min to remove fine MMT. Both the final precipitate and combined supernatant were freeze-dried (VirTis AdVantage Plus EL-85 Benchtop Freeze-Dryer, SP Scientific Inc., Gardiner, NY, USA). The lyophilized samples were collected and stored at −20 °C in a freezer until further characterization. Coating experiments were conducted in duplicate.

Determination of Amount of Protein Coated on MMT. The above lyophilized supernatant samples were dissolved in 10 mM NaH_2PO_4 buffer at pH 9.0 for determination of unbound protein using the bicinchoninic acid (BCA) method. The percentage of unbound protein was then calculated by normalization to the total protein used in coating, also measured using the BCA method. The BCA Protein Assay Reagent A was from Pierce Biotechnology, whereas Reagent B (4% w/v cupric sulfate) was laboratory-prepared. The incubation was at 37 °C for 30 min, and the absorbance was measured at 562 nm by using a UV−vis spectrophotometer (model Biomate 5, Thermo Electron Corp., Woburn, MA, USA). BSA was applied as a reference in establishing a standard curve. Triplicate tests were performed for each sample.

The amount of bound protein, in the lyophilized clay precipitate (coated MMT) samples from coating experiments, was determined for the total nitrogen content using the Dumas method[28] by Atlantic MicroLab, Inc. (Norcross, GA, USA). The nitrogen content was converted to protein content by multiplying with the Jones' factor, 6.25 for SP.[29] The percentage of bound protein was then estimated after dividing by the total protein used in coating. For consistency, the protein content of SPP in this estimation was also determined according to the Dumas method.

Determination of Protein Solubility. SPP was hydrated in 10 mM NaH_2PO_4 buffer with 4 mM NaCl to a final concentration of 1 mg/mL and adjusted to pH 2.0−10.0 using 1 N HCl or NaOH. The 4 mM NaCl was equivalent to the free sodium ion concentration in 1% w/v MMT dispersion estimated by using atomic absorption spectroscopy at the Department of Plant Sciences, University of Tennessee (Knoxville, TN, USA). After centrifugation at 10000g for 30 min, the supernatant was determined for protein concentration using the above BCA method. The protein solubility was then calculated as the percentage of protein remaining in the supernatant with respect to the total protein estimated according to the Dumas method.

Zeta Potential. The final precipitate in the above coating experiments was suspended in the phosphate buffer, adjusted to pH 2.0−10.0 using 1 N HCl or NaOH, and measured for zeta potential using a Delsa Nano C Zeta Potential/Particle Size Analyzer (Beckman Coulter, Fullerton, CA, USA). To characterize zeta potential of the bare MMT under coating conditions, 1% w/v MMT was suspended in phosphate buffer, adjusted for pH, heated and stirred for 3 h at 60 °C, and cooled to room temperature before testing. Triplicate measurements were conducted for each sample. Each measurement included 5 runs, each run for 10 cycles.

Wide-Angle X-ray Diffraction (XRD). An X-ray diffractometer (model X'Pert, PANalytical Inc., Westborough, MA, USA) with a generator voltage of 40 kV, a current of 40 mA, and a wavelength of 1.54 Å was used to conduct XRD analyses at 23 °C. The XRD patterns were obtained in the 2θ angle range of 2−12° in a fixed time mode with an increment of 0.02°, and plots were processed using the X'Pert Data Viewer software (PANalytical Inc.). Peak positions and d-spacing, calculated according to the Bragg equation (eq 1),[30] were determined directly by using the X'Pert HighScore Plus software (PANalytical Inc.). The experimental limit of detectable d-spacing in this study was also calculated using eq 1.[6,19] at a 2θ angle of 2°

$$d = \frac{\lambda}{2\sin(\theta)} \quad (1)$$

where λ is the wavelength of the X-ray beam and θ is the angle of the incident X-ray beam.

Fourier Transform Infrared Spectroscopy (FTIR). A powder potassium bromide (KBr) pellet method[8,31] was applied in FTIR experiments. A mixture of 1 mg of sample and 100 mg of KBr was ground to fine powder that was then pressed to a clear or translucent pellet loaded onto the instrument. The percent transmittance was collected at a wavenumber range of 4000−400 cm^{-1} using a model Nicolet 670 spectrometer (Thermo Nicolet, Madison, WI, USA). A pristine KBr pellet was used as background.

Statistical Analyses. Significant difference analyses were carried out with a least-significant difference ($P < 0.05$) mean separation method. Analyses were performed using SAS software (v. 9.3, SAS Institute Inc., Cary, NC, USA).

RESULTS AND DISCUSSION

Structures of MMT Coated by SP at Different pH Conditions. *XRD.* XRD patterns of pristine MMT and SPP are presented in Figure 1. Pristine MMT had a sharp characteristic peak at a 2θ angle of 7.11° with a d-spacing value of 1.24 nm,

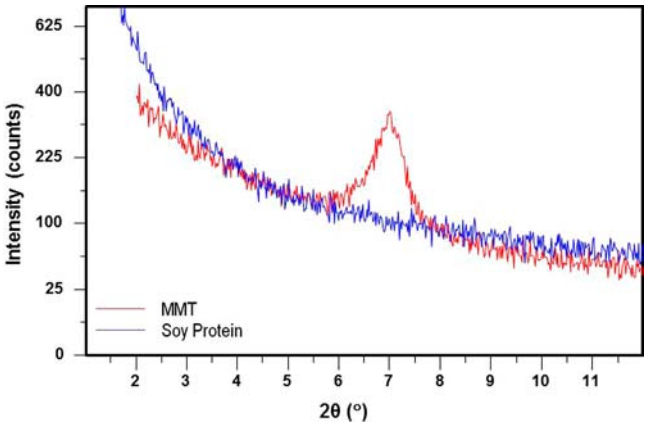

Figure 1. XRD patterns of pristine MMT and soy protein powder. The 2θ angle for MMT peak is 7.11°, with d-spacing of 1.24 nm.

consistent with the literature,[9,19] whereas SPP did not have any diffraction peaks in the studied 2θ range.

Figure 2 shows the XRD patterns of MMT samples coated at pH 2.0−10.0 with a MMT/SPP mass ratio of 4:1. Table 1 lists the d-spacing values of corresponding samples. A very weak peak was observed at pH 2.0, corresponding to a d-spacing value of 1.33 nm. At pH 3.0−5.0, sharp peaks appeared at 2θ angles of 6.63−7.08°, close to the characteristic peak for pristine MMT (Figure 1), and the d-spacing values were around 1.25−1.27 nm, slightly smaller than that at pH 2.0. At pH 6.0 or 7.0, two peaks were detected at 2θ of ca. 4.3 and 6.9°, corresponding to d-spacing values of 2.09 and 1.27 nm at pH 6.0, and 2.01 and 1.27 nm at pH 7.0. Humps with low onset of ca. 3° and 2θ angle of ca. 4.2−4.4° were observed for MMT coated by protein at pH 8.0−10.0, without the sharp peak of pristine MMT, corresponding to d-spacing values of 1.99−2.12 nm (Table 1). When bare MMT was similarly treated at coating conditions without SPP, XRD patterns did not demonstrate any changes (data not shown).

The shifting of the diffraction peak to a smaller 2θ angle, the left-shift, and increased d-spacing are characteristics of intercalated layer structures.[19] A greater extent of the left shift corresponds to a bigger d-spacing value. Thus, the pH 9.0 treatment resulted in more intercalated MMT structures than other pH treatments. When analyzed using two-dimensional sodium dodecyl sulfate−polyacrylamide gel electrophoresis (results not shown), most proteins corresponded to pI of 4.4−5.1 and molecular weight of 15−100 kDa, consistent with the literature.[32,33] Therefore, at pH 2, SP carries more positive charges than at other pH conditions, which facilitates the adsorption onto negatively charged MMT by electrostatic attraction. For samples at pH 6.0 and 7.0, the existence of two peaks implies the occurrence of partially intercalated MMT. At pH 8.0−10.0, broad peaks at low onset of ca. 3° imply a high extent of intercalated MMT structures.[30] Therefore, XRD patterns in Figure 2 indicate that intercalation of MMT occurred after coating by SP at all pH conditions, but the extent was pH-dependent.

FTIR. FTIR spectra of pristine MMT and SPP are demonstrated in Figure 3. Characteristic peaks of proteins appeared at wavenumbers of 2925, 2855, 1618−1681, 1530−1550, 1244, and 1450−1400 cm^{-1}. The former five peaks are due to absorbance by functional groups of $-CH_2$, $-CH$ (C—H stretching), amide I band (C═O stretching vibration), amide II band (N—H bending and C—N stretching modes), and

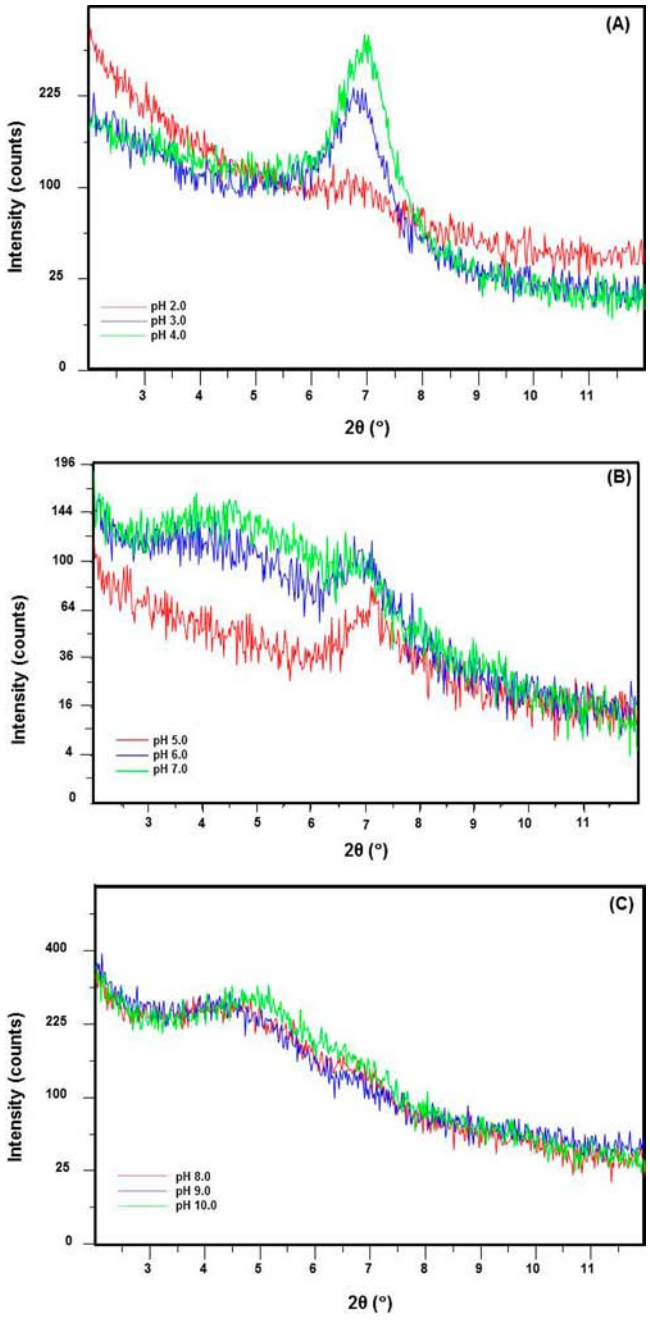

Figure 2. XRD patterns of MMT coated by soy protein using an MMT/soy protein powder mass ratio of 4:1 at (A) pH 2.0−4.0, (B) pH 5.0−7.0, and (C) pH 8.0−10.0.

amide III band, involving possible structures of $-CO—NH_2$, $-CO—NH-$, and/or $-CO—N-$.[18,34,35] The double peaks at 1450−1400 cm^{-1} are related with carboxyl (at approximately 1450 cm^{-1}) and carboxylate groups (at ca. 1410 cm^{-1}).

Figure 4 shows the FTIR spectra of MMT after coating by SP at different pH conditions. The presence of peaks corresponding to wavenumbers of 2925, 2855, 1618−1681, and 1530−1550 cm^{-1} confirms the coating of MMT by SP, as shown for changes of XRD patterns. The peak of SPP at 1244 cm^{-1} (Figure 3) disappeared after coating MMT (Figure 4), demonstrating changes of protein secondary structures such as contents of α-helix and β-sheet.[26,35] Peaks at wavenumbers of 1450−1400 cm^{-1} varied for samples coated at different pH conditions, whereas peaks at 1410 cm^{-1} disappeared for the

dx.doi.org/10.1021/jf301934j | J. Agric. Food Chem. 2012, 60, 11965−11971

Table 1. Basal Spacing of MMT after Coating by Soy Protein at an MMT/Soy Protein Powder Mass Ratio of 4:1 and pH 2.0−10.0

coating pH	2θ (deg)	d-spacing (nm)
2.0	6.63	1.33
3.0	7.07	1.25
4.0	6.96	1.27
5.0	7.08	1.25
6.0	4.23	2.09
	6.93	1.27
7.0	4.37	2.01
	6.98	1.27
8.0	4.30	2.05
9.0	4.16	2.12
10.0	4.43	1.99

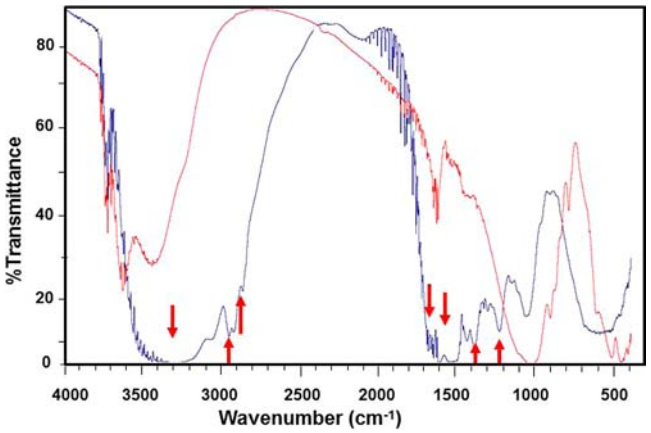

Figure 3. FTIR spectra of pristine MMT (red) and soy protein powder (blue). Arrows highlight positions discussed in the text.

ones at acidic pH values, but strengthened at alkaline pH values, illustrating more carboxylate groups formed at more basic conditions. Changes in relative intensities of the double peaks, that is, the ratio of carboxyl to carboxylate groups, additionally indicate changes of protein structure after adsorption on MMT.[26,35]

In addition, more hydrogen bonds formed at lower pH, demonstrated by broader peaks at wavenumbers of 3550−3230 cm^{-1} that are characteristic of hydroxyl group.[18] Hydrogen bonds can be formed between Si−O−Si and −OH groups of MMT and polar groups of proteins such as amide. The Si−O absorbance band occurs at wavenumbers of ∼1120−1014 cm^{-1}, and the disordering of clay platelets results in the intensity increase.[18] The broad peaks at wavenumbers of both ∼3550−3230 and ∼1120−1014 cm^{-1} in Figure 4A illustrate the significance of hydrogen bonding between MMT platelets and SP at highly acidic conditions.

Total Protein Coated on MMT. The amount of SP coating MMT was estimated by both the percentages remaining in the supernatant and those in the precipitate (Table 2). Despite discrepancy, the two methods, estimated by different protein assay methods, showed >90% protein bound with MMT, and there was no apparent trend of pH impact. Furthermore, although Table 2 shows the lowest solubility at pH 4.0, the amount of protein binding MMT was not the smallest. The two major SP fractions, glycinin and β-conglycinin, are composed of subunits. Glycinin has six acidic subunits of ca. 35 kDa and six basic units of ∼20 kDa,[36] whereas β-conglycinin is a trimer

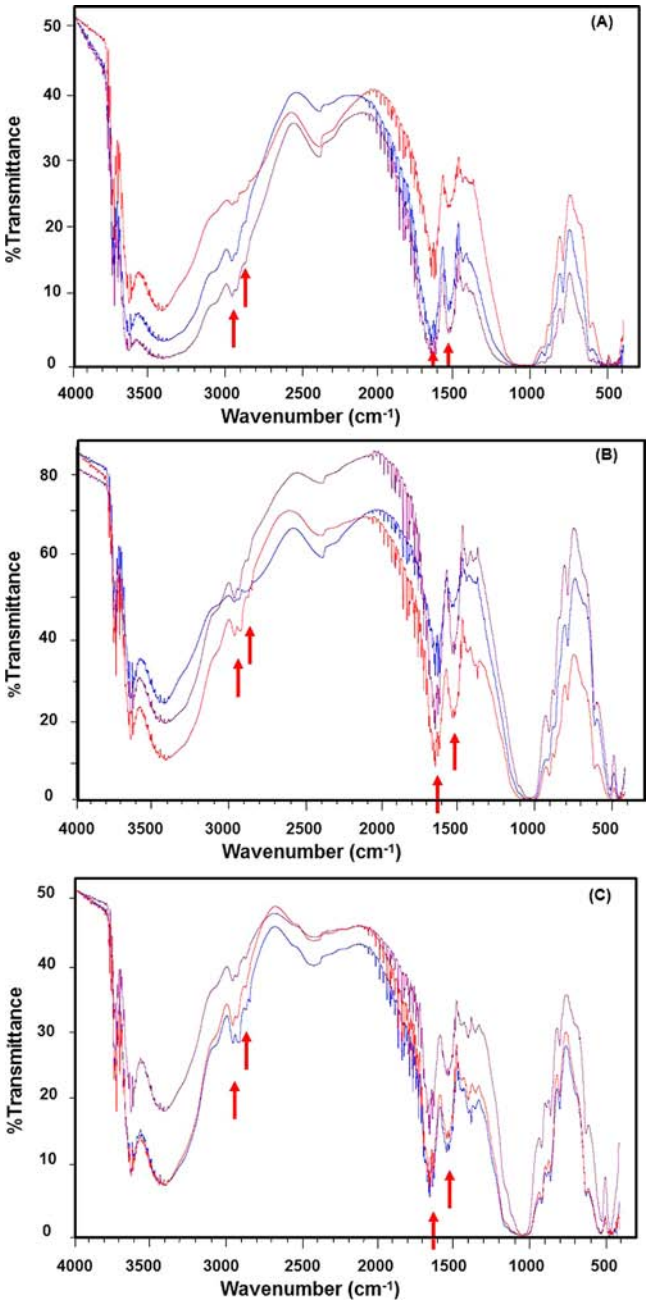

Figure 4. FTIR spectra of MMT coated by soy protein at an MMT/soy protein powder mass ratio of 4:1 and (A) pH 2.0 (blue), 3.0 (purple), and 4.0 (red), (B) pH 5.0 (blue), 6.0 (purple), and 7.0 (red), and (C) pH 8.0 (blue), 9.0 (purple), and 10.0 (red). Arrows highlight positions discussed in the text.

corresponding to 60, 67, and 71 kDa.[37] The association and dissociation of these subunits are dependent on pH, temperature, reducing agents, etc.,[36,37] and likely affect the coating results. It however should be noted that charged patches on the protein surface may allow binding with polyelectrolytes that have the same type of net charge as proteins.[38] The pK_a values of the side chain of cysteine, lysine, tyrosine, and arginine are 8.4, 10.5, 10.5, and 12.5, respectively, reflecting contents of 1.26, 6.23, 3.81, and 7.90 g/100 g protein in SP isolate, respectively.[39] Because charged amino acid residues are mostly located on the surface of protein molecules,[40] these basic amino acid residues can carry positive charges at basic conditions to

dx.doi.org/10.1021/jf301934j | J. Agric. Food Chem. 2012, 60, 11965−11971

Table 2. Impact of pH on Soy Protein Solubility and Binding onto MMT at an MMT/Soy Protein Powder Mass Ratio of 4:1

pH	protein solubility[a] (%)	unbound protein[a] (%)	bound protein[b] (%)
2.0	86.70 ± 0.29abc	0.72 ± 0.005G	100.00 ± 1.68bc
3.0	83.24 ± 0.61e	0.80 ± 0.01F	105.09 ± 2.33a
4.0	75.49 ± 1.91f	0.55 ± 0.01H	93.91 ± 1.34cd
5.0	83.48 ± 1.79de	0.71 ± 0.01G	106.71 ± 2.48a
6.0	85.39 ± 1.05bcde	1.15 ± 0.01D	103.11 ± 1.84ab
7.0	84.68 ± 0.51cde	0.95 ± 0.02E	97.64 ± 2.58bc
8.0	86.23 ± 0.62abcd	2.18 ± 0.04A	90.19 ± 2.44d
9.0	88.13 ± 0.68ab	1.85 ± 0.03B	93.29 ± 2.89cd
10.0	89.09 ± 0.57a	1.60 ± 0.03C	92.80 ± 2.07cd

[a]Different letters in the column indicate significant difference ($P < 0.001$). Numbers are the average ± standard deviation from three measurements using the BCA method. [b]Different letters in this column indicate significant difference ($P < 0.001$). Numbers are the average ± standard deviation from duplicate measurements using the Dumas method.

provide sites for adsorption on negatively charged MMT. Nevertheless, the protein adsorption data again suggests the significance of both coulumbic (opposite charges) and noncoulumbic forces.

Zeta Potential. As shown in Figure 5, bare MMT had negative charges at all pH conditions. Zeta-potential values of

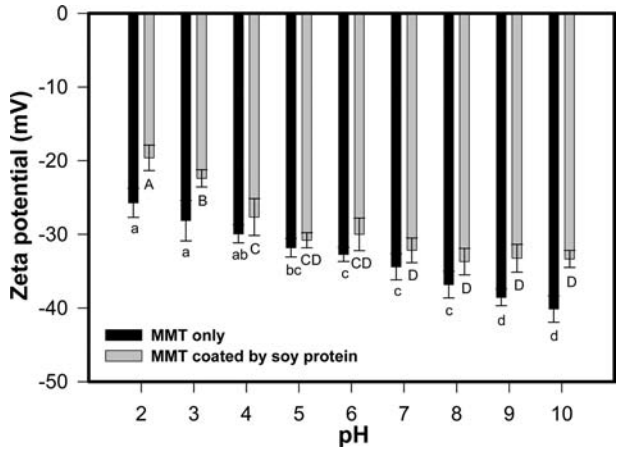

Figure 5. Comparasion of zeta potential of bare MMT dispersion in 10 mM NaH_2PO_4 buffer and soy protein-coated MMT at pH 2.0–10.0. Coating was conducted at an MMT/soy protein powder mass ratio of 4:1. Error bars are standard deviations for duplicate coating experiments, each measured three times. Different letters in each group (bare and protein-coated MMT) indicate significant difference ($P < 0.001$).

the SP-coated MMT were less negative than those of bare ones. The zeta potential of SP is between about +30 and −40 mV at pH 2.0–8.0, with a value of 0 at pH ~4.6 (p*I*).[41,42] Below p*I*, SP is positively charged, and the adsorption of SP on MMT is expected to lower the zeta potential of MMT, which is more apparent at lower pH values. Above p*I*, SP is overall negatively charged but adsorbs on MMT for >90% (Table 2), resulting in the reduced magnitude of negative zeta potential of MMT that did not show significant dependence on pH (Figure 5). The adsorption due to both coulumbic and noncoulumbic mechanisms, as discussed above, is reflected by the reduced magnitude of negative zeta potential of MMT after coating.

Effect of MMT/SPP Mass Ratio on MMT Structure Coated by SPP at pH 9.0. Because pH 9.0 was used in extraction, verified for good solubility of SP (Table 2), and corresponded to the largest *d*-spacing (Table 1), this pH was used to study the impact of MMT/SPP mass ratios, shown in Figure 6 for XRD patterns and Table 3 for *d*-spacing values.

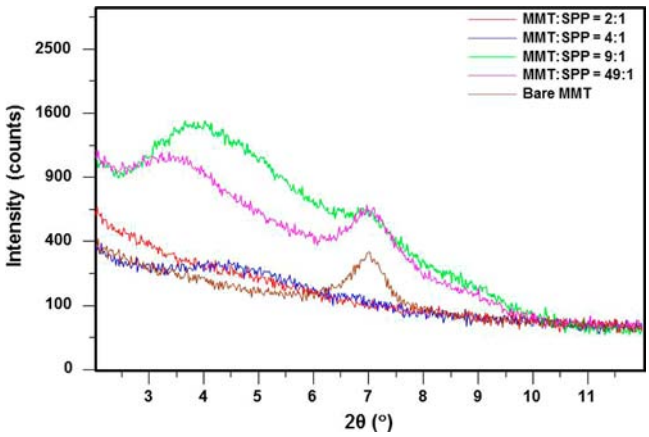

Figure 6. XRD patterns of pristine MMT (brown curve) and MMT coated by soy protein at MMT/soy protein powder (SPP) mass ratios of 2:1 (red), 4:1 (blue), 9:1 (green), and 49:1 (pink) at pH 9.0. The curves at the 4:1 mass ratio and pristine MMT are repeated here for convenience of comparison.

Table 3. XRD Characteristics of MMT Coated by Soy Protein at pH 9.0 Using Different MMT/Soy Protein Powder (SPP) Mass Ratios, with Comparison to Simple Mixtures of MMT and SPP

	MMT/SPP mass ratio	2θ (deg)	*d*-spacing (nm)
coated sample	2:1	not detectable	not detectable
	4:1	4.16	2.12
	9:1	3.84	2.30
		7.13	1.24
	49:1	3.35	2.64
		6.91	1.26
simple mixture	2:1	7.29	1.21
	4:1	7.06	1.25
	9:1	6.98	1.27
	49:1	6.90	1.28

Two diffraction peaks were detected for samples prepared with MMT/SPP mass ratios of 49:1 and 9:1: one similar to that of the pristine MMT and the other showing a left-shift to a lower 2θ angle. The corresponding *d*-spacing values were 2.30 and 1.24 nm at the mass ratio of 9:1 and 2.64 and 1.27 nm at the mass ratio of 49:1. When compared to a single peak at a mass ratio of 4:1, as discussed above, the insufficient amount of SP at MMT/SPP mass ratios of 49:1 and 9:1 enabled only partial intercalation of MMT platelets. When the MMT/SPP mass ratio was lowered to 2:1, the diffraction peak of pristine MMT, at 2θ of 7.11°, was no longer detected. The disappearance of the diffraction peak characteristic of pristine MMT generally can be caused by the formation of either fully exfoliated or highly intercalated structures that are beyond the detection

limit of the set 2θ range,[6] which was 2° in this study, corresponding to a *d*-spacing value of 4.41 nm.

To clarify that the disappearance of diffraction peak characteristic of the pristine MMT was not caused by dilution with SPP,[30] simple mixtures of MMT and SPP at mass ratios from 2:1 to 49:1 were also characterized by XRD. All mixtures demonstrated a peak corresponding to a 2θ angle of 6.9−7.3° (Figure 7) with *d*-spacing values of 1.21−1.28 nm (Table 3),

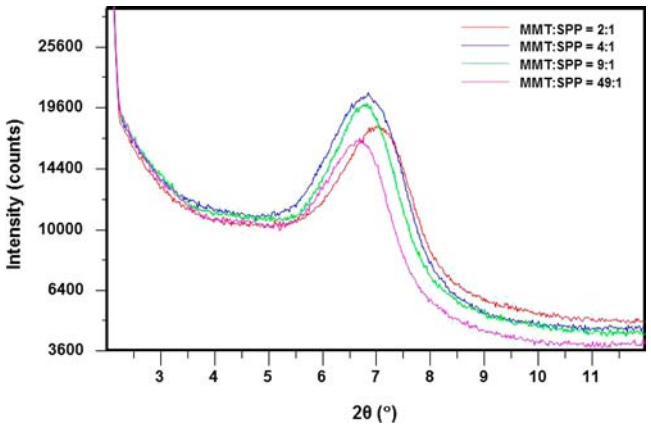

Figure 7. XRD patterns of simple mixtures of MMT and soy protein powder (SPP) at MMT/SPP mass ratios of 2:1 (red), 4:1 (blue), 9:1 (green), and 49:1 (pink).

very similar to those of pristine MMT (Figure 3). Thus, XRD patterns of coated MMT are due to intercalation and/or exfoliation of platelets, and the larger *d*-spacing at a smaller MMT/SPP mass ratio, that is, a higher protein level, is likely caused by increased possibility for protein chains to penetrate into MMT galleries to separate clay platelets.[19] The results from XRD have been repeatedly verified by structures assessed by transmission electron microscopy[19,30] that was thus not attempted in this study.

This group of samples was also characterized for FTIR that had similar features as discussed previously (data not shown), verifying the presence of proteins on MMT after coating. Similarly, zeta potential was measured for samples prepared with various MMT/SPP mass ratios (Figure 8). A higher SPP

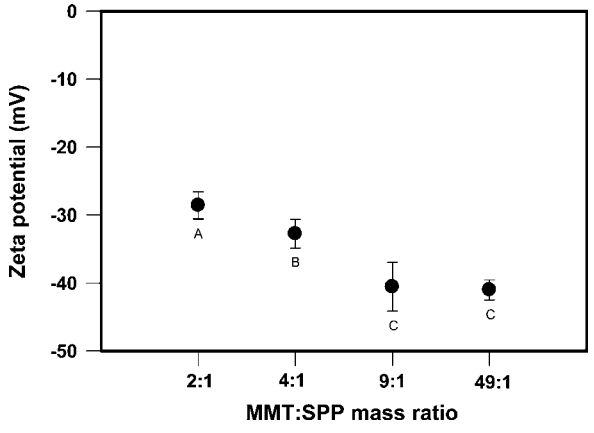

Figure 8. Zeta potential of MMT coated by soy protein at pH 9.0 using various MMT/soy protein powder (SPP) mass ratios. Error bars are standard deviations from duplicate coating experiments, each measured three times. Different letters next to symbols indicate significant difference ($P < 0.001$).

mass level corresponded to a less negative zeta potential, indicating an increased amount of SP adsorbing on MMT. This study strengthens the conclusion that protein adsorption on MMT involves both coulumbic and noncoulumbic forces.

In summary, MMT was modified from highly ordered to highly intercalated or fully exfoliated structures after surface coating by a sufficient amount of SP. The percentage of protein binding on MMT exceeded 90% at a MMT/SPP mass ratio of 4:1, regardless of coating pH conditions. The binding was caused by both electrostatic attraction and noncoulumbic forces such as hydrogen bonding between MMT and SP, which was verified by complementary results from XRD, FTIR, zeta-potential analysis, and quantification of amounts of unbound and bound proteins. The present study thus demonstrated that intercalation/exfoliation of MMT can be easily achieved by coating using low-cost SP. The practical approach can be integrated in preparations of various nanocomposite materials.

AUTHOR INFORMATION

Corresponding Author

*Postal address: Department of Food Science and Technology, The University of Tennessee, 2605 River Drive, Knoxville, TN 37996, USA. Phone: 1 (865) 974-6196. Fax: 1 (865) 974-7332. E-mail: qzhong@utk.edu.

Funding

The project was supported by the University of Tennessee and the U.S. Department of Agriculture under Project KS601076.

Notes

The authors declare no competing financial interest.

ACKNOWLEDGMENTS

We thank Dr. Carl Sams for assisting in experiments in atomic absorption spectroscopy.

REFERENCES

(1) Sorrentino, A.; Gorrasi, G.; Vittoria, V. Potential perspectives of bio-nanocomposites for food packaging applications. *Trends Food Sci. Technol.* **2007**, *18*, 84−95.

(2) Zhao, R. X.; Torley, P.; Halley, P. J. Emerging biodegradable materials: starch- and protein-based bio-nanocomposites. *J. Mater. Sci.* **2008**, *43*, 3058−3071.

(3) The global outlook for biodegradable packaging. *Business Insights* 2011, *June*, 110; http://www.researchandmarkets.com/research/5e27e0/the_global_outlook.

(4) Marsh, K.; Bugusu, B. Food packaging − roles, materials, and environmental issues. *J. Food Sci.* **2007**, *72*, R39−R55.

(5) Arora, A.; Padua, G. W. Review: nanocomposites in food packaging. *J. Food Sci.* **2010**, *75*, R43−R49.

(6) Dang, Q. Q.; Lu, S. D.; Yu, S.; Sun, P. C.; Yuan, Z. Silk fibroin/montmorillonite nanocomposites: effect of pH on the conformational transition and clay dispersion. *Biomacromolecules* **2010**, *11*, 1796−1801.

(7) de Azeredo, H. M. C. Nanocomposites for food packaging applications. *Food Res. Int.* **2009**, *42*, 1240−1253.

(8) Gunister, E.; Pestreli, D.; Unlu, C. H.; Atici, O.; Gungor, N. Synthesis and characterization of chitosan-MMT biocomposite systems. *Carbohydr. Polym.* **2007**, *67*, 358−365.

(9) Essington, M. E. *Soil and Water Chemistry: An Intergrative Approach*; CRC Press: Boca Raton, FL, 2003; pp 58, 65, 68.

(10) Cuq, B.; Gontard, N.; Guilbert, S. Proteins as agricultural polymers for packaging production. *Cereal Chem.* **1998**, *75*, 1−9.

(11) Kumar, P.; Sandeep, K. P.; Alavi, S.; Truong, V. D.; Gorga, R. E. Preparation and characterization of bio-nanocomposite films based on soy protein isolate and montmorillonite using melt extrusion. *J. Food Eng.* **2010**, *100*, 480−489.

(12) Paetau, I.; Chen, C. Z.; Jane, J. L. Biodegradable plastics made from soybean products. 1. Effect of preparation and processings on mechanical-properties and water-absorption. *Ind. Eng. Chem. Res.* **1994**, *33*, 1821−1827.
(13) Xiang, L. X.; Tang, C. Y.; Cao, J.; Wang, C. Y.; Wang, K.; Zhang, Q.; Fu, Q.; Zhao, S. G. Preparation and characterization of soy protein isolate (SPI)/montmorillonite (MMT) bionanocomposites. *Chinese J. Polym. Sci.* **2009**, *27*, 843−849.
(14) Kumar, P.; Sandeep, K. P.; Alavi, S.; Truong, V. D.; Gorga, R. E. Effect of type and content of modified montmorillonite on the structure and properties of bio-nanocomposite films based on soy protein isolate and montmorillonite. *J. Food Sci.* **2010**, *75*, N46−N56.
(15) Cao, N.; Fu, Y. H.; He, J. H. Preparation and physical properties of soy protein isolate and gelatin composite films. *Food Hydrocolloids* **2007**, *21*, 1153−1162.
(16) Krochta, J. M.; DeMulderJohnston, C. Edible and biodegradable polymer films: challenges and opportunities. *Food Technol.* **1997**, *51*, 61−74.
(17) Song, F.; Tang, D. L.; Wang, X. L.; Wang, Y. Z. Biodegradable soy protein isolate-based materials: a review. *Biomacromolecules* **2011**, *12*, 3369−3380.
(18) Chen, P.; Zhang, L. Interaction and properties of highly exfoliated soy protein/montmorillonite nanocomposites. *Biomacromolecules* **2006**, *7*, 1700−1706.
(19) Tang, X. Z.; Alavi, S.; Herald, T. J. Barrier and mechanical properties of starch-clay nanocomposite films. *Cereal Chem.* **2008**, *85*, 433−439.
(20) Le Corre, D.; Bras, J.; Dufresne, A. Starch nanoparticles: a review. *Biomacromolecules* **2010**, *11*, 1139−1153.
(21) Yang, Y.; Zhu, Z. K.; Yin, J.; Wang, X. Y.; Qi, Z. E. Preparation and properties of hybrids of organo-soluble polyimide and montmorillonite with various chemical surface modification methods. *Polymer* **1999**, *40*, 4407−4414.
(22) Feng, M.; Zhao, C. G.; Gong, F. L.; Yang, M. S. Study on the modification of sodium montmorillonite with amino silanes. *Acta Chim. Sinica* **2004**, *62*, 83−87.
(23) Mallakpour, S.; Dinari, M. Preparation and characterization of new organoclays using natural amino acids and Cloisite Na(+). *Appl. Clay Sci.* **2011**, *51*, 353−359.
(24) Lin, J. J.; Wei, J. C.; Juang, T. Y.; Tsai, W. C. Preparation of protein−silicate hybrids from polyamine intercalation of layered montmorillonite. *Langmuir* **2007**, *23*, 1995−1999.
(25) Ding, X. L.; Henrichs, S. M. Adsorption and desorption of proteins and polyamino acids by clay minerals and marine sediments. *Mar. Chem.* **2002**, *77*, 225−237.
(26) Quiquampoix, H.; Burns, R. G. Interactions between proteins and soil mineral surfaces: environmental and health consequences. *Elements* **2007**, *3*, 401−406.
(27) L'Hocine, L.; Boye, J. I.; Arcand, Y. Composition and functional properties of soy protein isolates prepared using alternative defatting and extraction procedures. *J. Food Sci.* **2006**, *71*, C137−C145.
(28) AOAC. *Official Methods of Analysis*, 17th ed.; Association of Official Analytical Chemists International: Gaithersburg, MD, 2000; Vol. *I*, Method 968.06, p 13.
(29) Mariotti, F.; Tome, D.; Mirand, P. P. Converting nitrogen into protein − beyond 6.25 and Jones' factors. *Crit. Rev. Food Sci. Nutr.* **2008**, *48*, 177−184.
(30) Kumar, P. *Development of Bio-nanocomposite Films with Enhanced Mechanical and Barrier Properties Using Extrusion Processing*; Ph.D. dissertation, North Carolina State University, 2009.
(31) Chen, P.; Tian, H. F.; Zhang, L.; Chen, Y.; Wang, X. Y.; Do, Y. M. Structure and properties of soy protein/alumina hydrate nanocomposites fabricated via *in situ* synthesis. *J. Biobased Mater. Bioenergy* **2008**, *2*, 248−257.
(32) Liu, S. H.; Zhou, R. B.; Tian, S. J.; Gai, J. Y. A study on subunit groups of soybean protein extracts under SDS-PAGE. *J. Am. Oil Chem. Soc.* **2007**, *84*, 793−801.
(33) Wu, W.; Zhang, C. M.; Kong, X. Z.; Hua, Y. F. Oxidative modification of soy protein by peroxyl radicals. *Food Chem.* **2009**, *116*, 295−301.
(34) Nakasato, K.; Ono, T.; Ishiguro, T.; Takamatsu, M.; Tsukamoto, C.; Mikami, M. Rapid quantitative analysis of the major components in soymilk using fourier transform infrared spectroscopy (FT-IR). *Food Sci. Technol. Res.* **2004**, *10*, 137−142.
(35) Servagent-Noinville, S.; Revault, M.; Quiquampoix, H.; Baron, M. H. Conformational changes of bovine serum albumin induced by adsorption on different clay surfaces: FTIR analysis. *J. Colloid Interface Sci.* **2000**, *221*, 273−283.
(36) Badley, R. A.; Atkinson, D.; Hauser, H.; Oldani, D.; Green, J. P.; Stubb, J. M. The structure, physical and chemical properties of the soy bean protein glycinin. *Biochim. Biophys. Acta* **1975**, *412*, 214−428.
(37) Maruyama, N.; Katsube, T.; Wada, Y.; Oh, M. H.; Barba De La Rosa, A. P.; Okuda, E.; Nakagawa, S.; Utsumi, S. The roles of the N-linked glycans and extension regions of soybean β-conglycinin in folding, assembly and structural features. *Eur. J. Biochem.* **1998**, *258*, 854−862.
(38) Dickinson, E. Hydrocolloids at interfaces and the influence on the properties of dipsersed systems. *Food Hydrocolloids* **2003**, *17*, 25−39.
(39) Hughes, G. J.; Ryan, D. J.; Mukherjea, R.; Schasteen, C. S. Protein digestibility-corrected amino acid scores (PDCAAS) for soy protein isolates and concentrate: criteria for evaluation. *J. Agric. Food Chem.* **2011**, *59*, 12707−12712.
(40) Tang, C. H.; Chen, L.; Ma, C. Y. Thermal aggregation, amino acid composition and in vitro digestibility of vicilin-rich protein isolates from three *Phaseolus* legumes: a comparative study. *Food Chem.* **2009**, *113*, 957−963.
(41) Malhotra, A.; Coupland, J. N. The effect of surfactants on the solubility, zeta potential, and viscosity of soy protein isolates. *Food Hydrocolloids* **2004**, *18*, 101−108.
(42) Liu, C.; Teng, Z.; Lu, Q. Y.; Zhao, R. Y.; Yang, X. Q.; Tang, C. H.; Liao, J. M. Aggregation kinetics and ζ-potential of soy protein during fractionation. *Food Res. Int.* **2011**, *44*, 1392−1400.